Supplementary Material

Multi-scale tomographic analysis for micron-sized particulate samples

Ralf Ditscherlein[1,*], Orkun Furat[2], Mathieu de Langlard[2], Juliana Martins de Souza e Silva[3], Johanna Sygusch[4], Martin Rudolph[4], Thomas Leißner[1], Volker Schmidt[2], and Urs A. Peuker[1]

[1]Institute of Mechanical Process Engineering and Mineral Processing, Technische Universität Bergakademie Freiberg, D-09599 Freiberg, Germany
[2]Institute of Stochastics, Ulm University, D-89069 Ulm, Germany
[3]Institute of Physics - mikroMD, Martin Luther University Halle-Wittenberg, D-06120 Halle, Germany
[4]Helmholtz Institute Freiberg for Resource Technology, D-09599 Freiberg, Germany
[*]corresponding author: ralf.ditscherlein@mvtat.tu-freiberg.de, phone: +49 3731 39-2714, fax: +49 3731 39-2947

Appendix A: Particle system

For validation purposes in image processing, a detailed preliminary characterization of the particle systems is mandatory. It enables us to quantify the accuracy of the proposed segmentation procedure and to account for eventual bias linked to the image processing workflow. Figure S1 shows cutouts of both analyzed particulate materials.

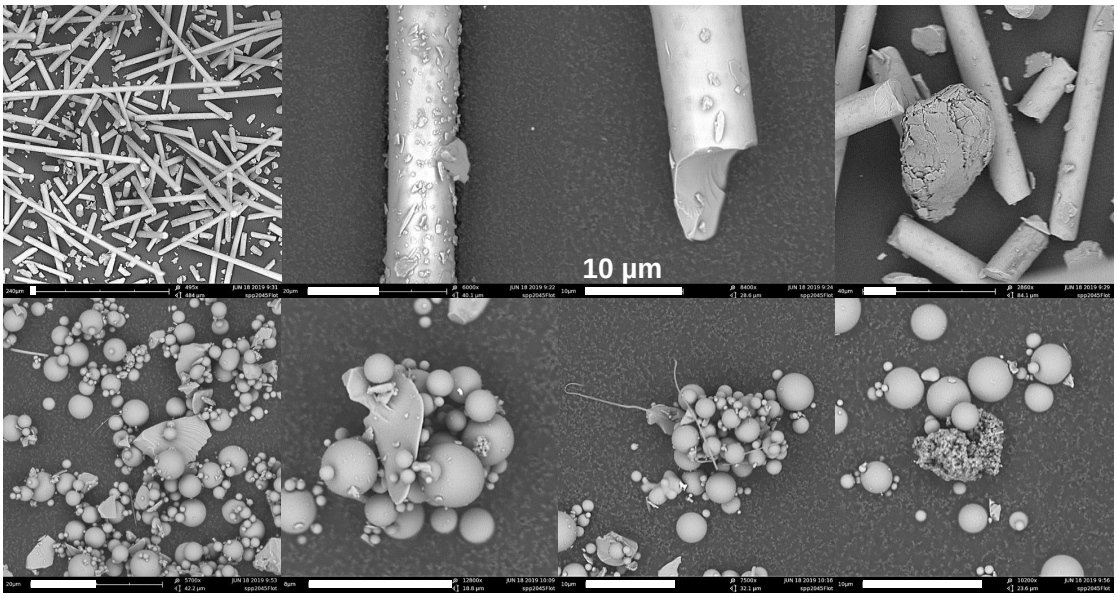

Figure S1: SEM-images of fibres (top) with contamination on the particle surface (organic facening from production process) and spheres (bottom). Note that these images are extreme examples and not representative for the analyzed particle system.

For a reasonable pre-characterization of both particle systems in terms of size (spheres: diameter, fibres: length) we used SEM and light microscopy 2D imaging methods. Integral methods like laser diffraction (in case of spherical systems) are also available but expected to be not comparable due to the different measurement principle. The workflow was as follows: (1) separate the particles on the object carrier, (2) take images at 10 random locations, (3) determine the size of each particle with the ROI-manager of ImageJ (exemplary images of spheres and fibres see Figure S2) and (4) combine all data sets.

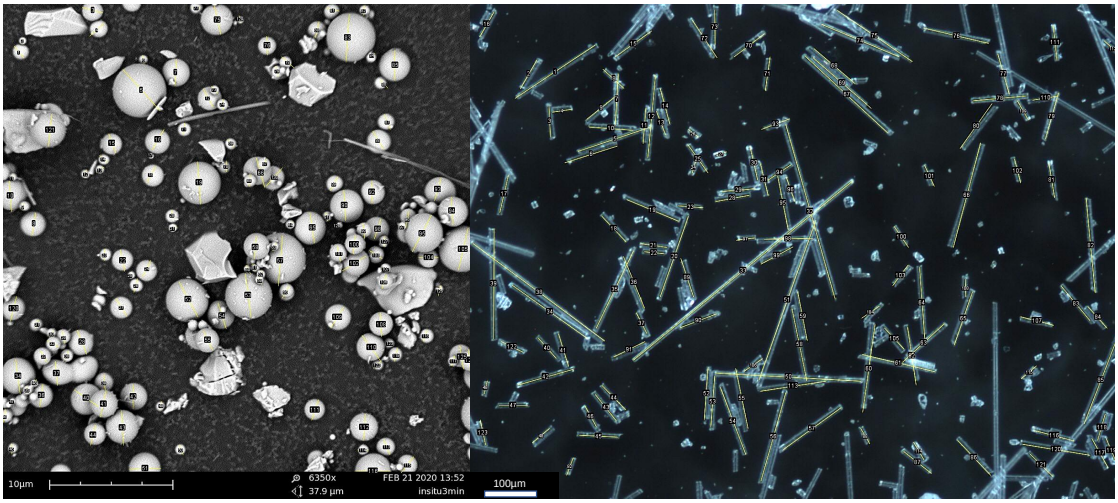

Figure S2: Exemplary SEM image showing the spheres (left) and exemplary image from light microscopy showing the fibres (right)

Table S1: Statistical measures for particle systems determined by 2D image analysis (spheres: SEM, fibres: light microscopy); (*) size is the equivalent spherical diameter, (**) diameter from data sheet specification: 10 µm

Measures	**Sphere diameter*** *in* µm	Fibre length** *in* µm
$Q_{0.10}$	0.6	40.8
$Q_{0.50}$	1.2	81.6
$Q_{0.90}$	2.9	208.7
Min	0.4	17.7
Max	5.8	656.9
Number of particles	1181	1371

The resulting statistical measures of both particle systems are summarized in Table S1. We refrained from automation, since overlay effects in the 2D representation make meaningful binarization and segmentation difficult and, in the case of fibres, lead to over-segmentation. The focus is clearly on 3D analysis.

Appendix B: Partial volume effect

To analyze the particle distribution of our system, we have to distinguish each particle from the background (in this study a wax matrix) and separate the agglomerated particles from each other. The relevant boundary layer (particle-matrix / particle-particle) extends only partially into the surrounding voxel layer. The resulting gray values of these voxels are a mixture between particle and matrix phase depending on their share (partial volume) in the voxel and their specific X-ray attenuation capability. Figure S3 shows an example of a reconstructed CT-image slice of spherical particles (a). Particles are aggregated (b,c-yellow) or physically connected/sintered (b,c-red). Segmenting the particles means finding the proper delimited regions such that each region corresponds to one particle. Gray blend pixels are assigned to either the particle (white) or the matrix (black), which is called binarization by thresholding. In both cases this has an influence on the number, size and shape of the resulting particles (compare d with e).

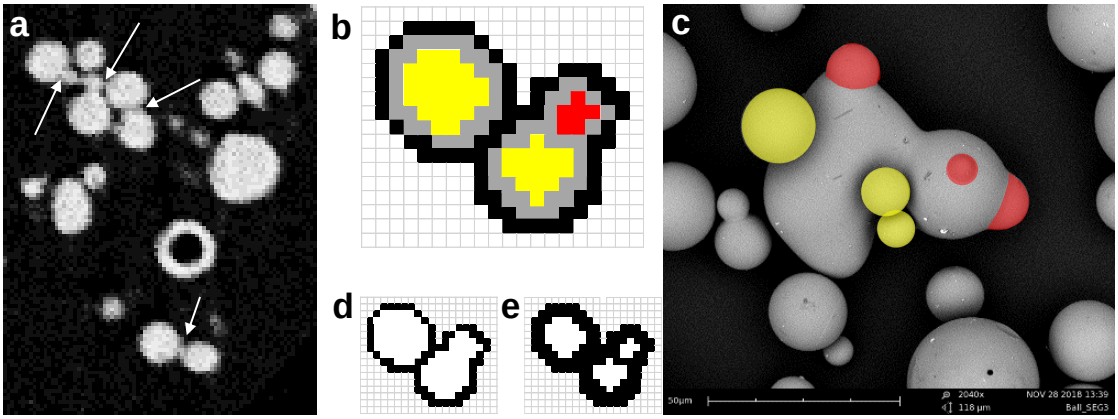

Figure S3: Magnification of a reconstructed tomographic slice (a) where connections between particles are marked (arrow), example of physically connected (b-red) and aggregated particles (b-yellow) with corresponding SEM-image (c), change in particle size, number and shape after thresholding (d,e)

The exemplary analysis of the sphere diameters clearly shows the influence of partial volume effect on the location and shape of the distribution (see Figure S4). Only in the high-resolution CT images are the spherical particles sufficiently well resolved to be able to depict their true size distribution.

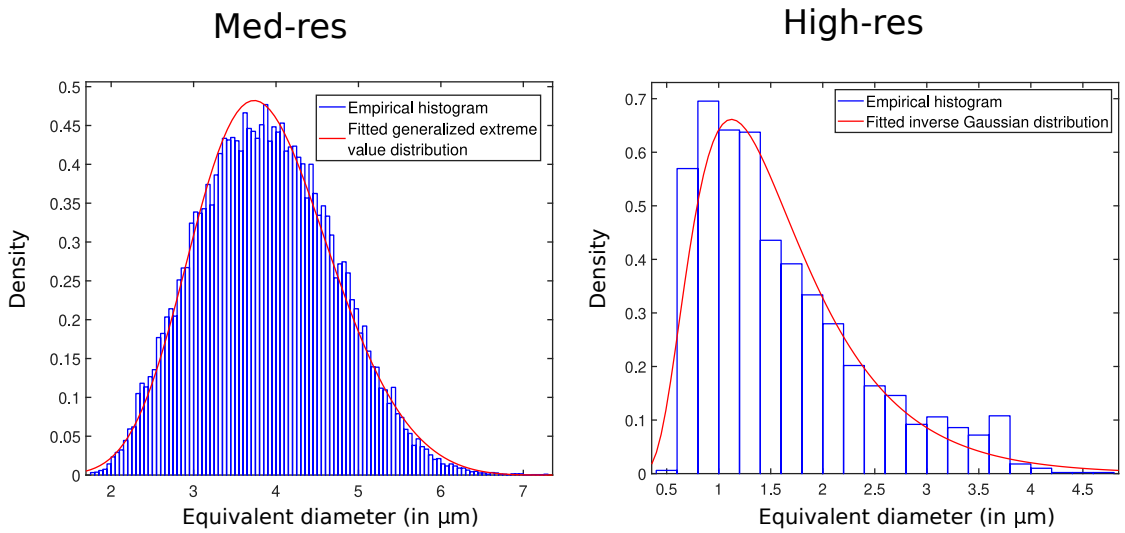

Figure S4: Comparison of the volume-equivalent diameter distributions computed from the med-res and high-res CT images.

Appendix C: Experimental setup

The main difference between micro- and nano-CT is the type of X-rays. In both cases X-rays are generated by the interaction between accelerated electrons with a specific target material (in our case micro-CT/Tungsten, nano-CT/Chromium).

In micro-CT imaging the whole spectrum of X-rays (characteristic and bremsstrahlung) is used as part of a conical beam that is generated by the interaction volume within the target material. So, each individual volume element of the sample material interacts with the whole energy-spectrum of X-rays and alters it. Because the detector is not energy-dispersive, every arriving X-ray photon counts as part of the sum signal. Both, the polychromatic spectrum and the conical beam shape, cause image artefacts.

In nano-CT imaging, a condensor lense filters a specific part of the spectrum and, in this way, creates approximately monochromatic X-rays in a parallel beam. Thus, there are much less artefacts. But because of the lower photon intensity, a much higher exposure time is needed to generate a sufficient signal on the detector. Inside views and corresponding measurement setups of both CT-scanners are visualized in Figure S5.

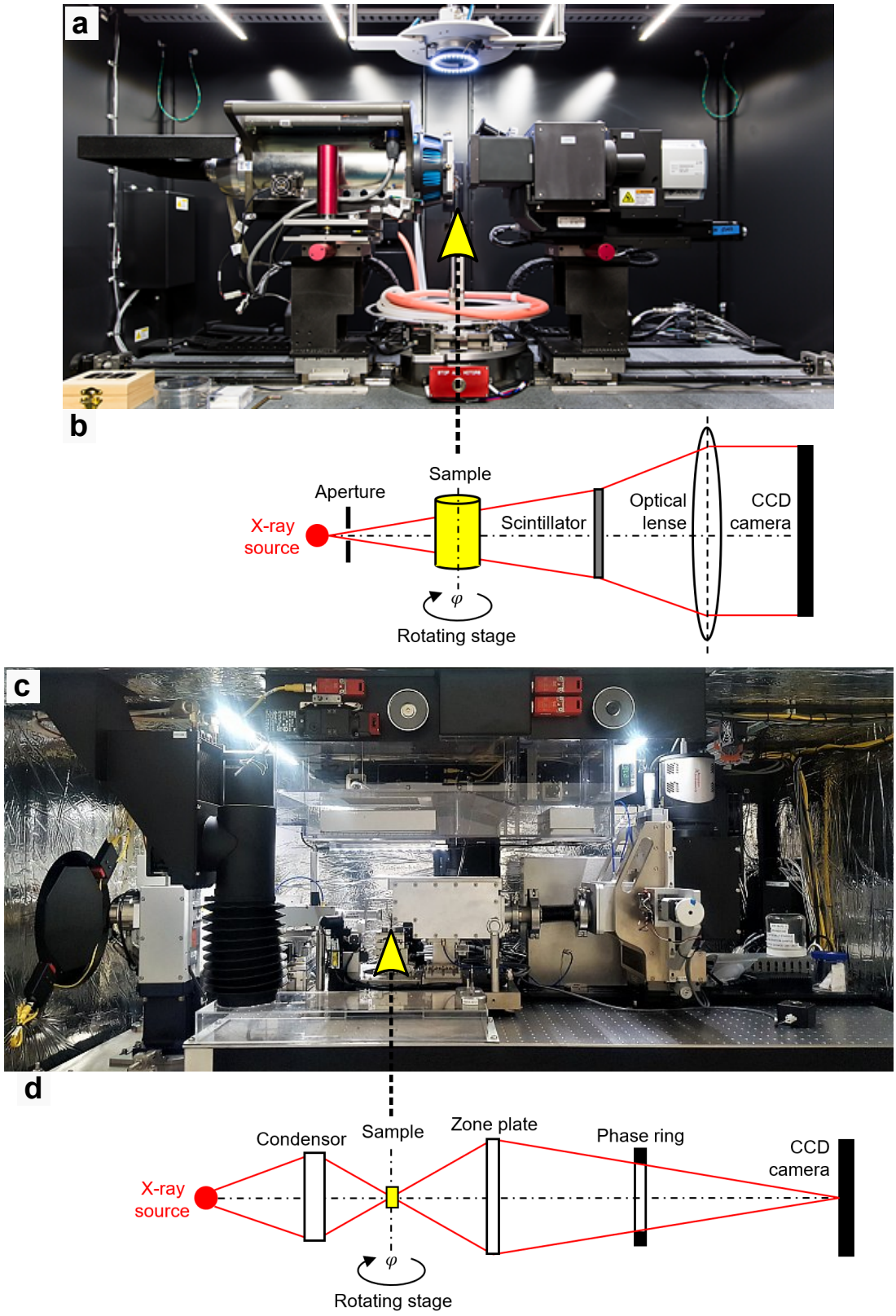

Figure S5: Inside view of micro-CT (a) and nano-CT (c), with corresponding measurement setups (b, d).

Appendix D: Region of interest (ROI) tomography

Ideally, the sample should be a little bit smaller than the field of view (FOV). Thus, when going to higher voxel-resolution, the sample size has to shrink. If this is not possible due to limited machining capabilities or simply because the sample should not be destroyed, the FOV is shifted inside the sample (Figure S6-a). This affects the minimum number of projections, needed for reconstruction, as discussed in the main part of the paper.

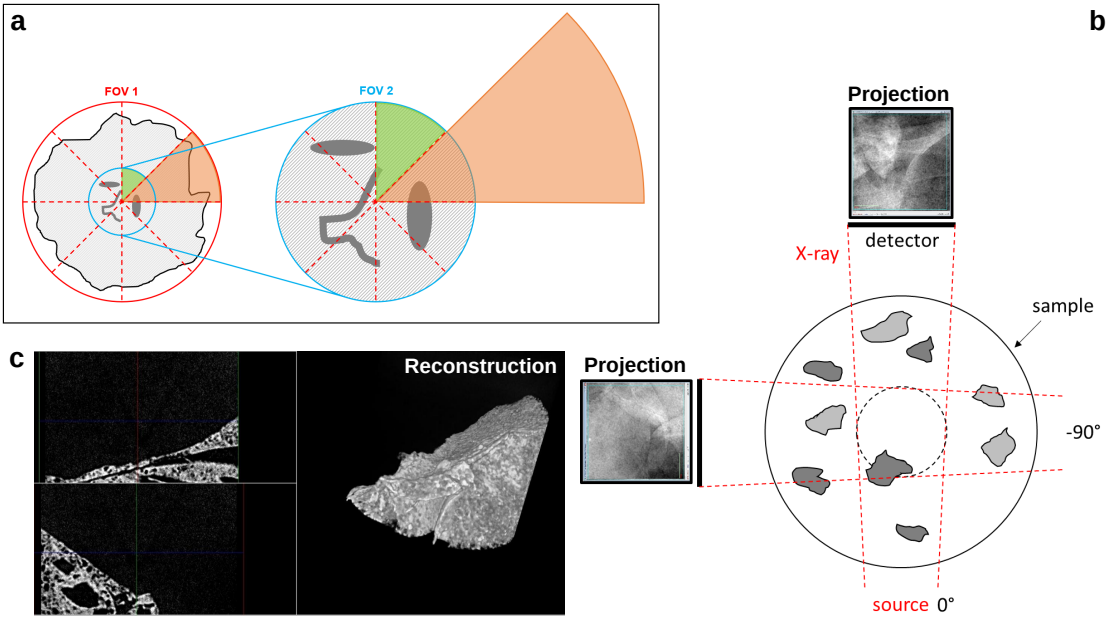

Figure S6: Comparison of two scans of the same sample – whole sample within the field of view (a, FOV1), detail enlargement by ROI (a, FOV2), possible ROI-identification problems (b,c)

ROI-tomography is also challenging in terms of searching for an appropriate scan volume with enough particles in it. Especially when looking for certain structures, the projection image does not tell us, whether the structures are inside the FOV. In this case a common solution is to make a low-quality pre-scan with a limited number of projections to search for the ROI. Afterwards, the determined coordinates are used for a high-resolution scan.

Appendix E: Multidimensional characterization of fibres

A cylindrical fibre is uniquely defined by its size d (height of the cylinder) and its cross-sectional diameter d_{cross}. Another process-relevant characteristic is its specific surface area

$$S_{V_p} = \frac{S}{V_p} = \frac{2d_{\text{cross}} + 4d}{d\, d_{\text{cross}}}. \tag{1}$$

The histograms of these characteristics and their parametric fits are depicted in Fig. S7a. Furthermore, Fig. S7b. visualizes the bivariate probability density of size and specific surface area using a bivariate histogram (left) and a parametric copula model (right).

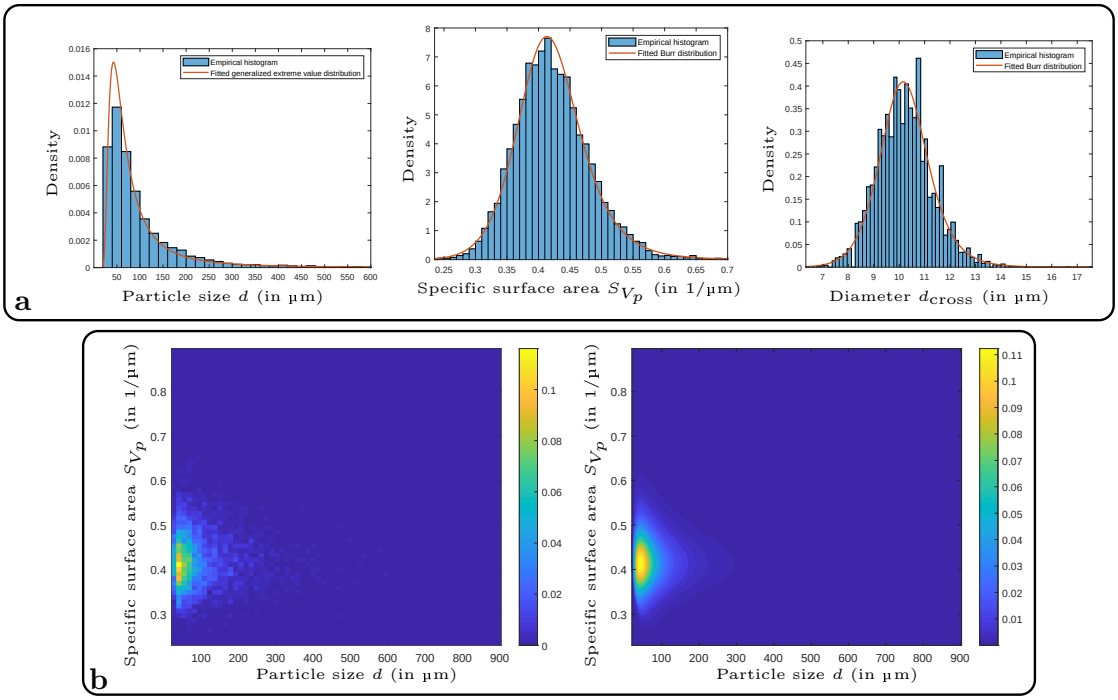

Figure S7: a) Fitted parametric (marginal) distributions to size (left), specific surface area (middle) and diameter (right) of fibres; b) bivariate histogram (left) and the fitted bivariate probability density using a BB8 copula (right).

Note that, instead of the size d and diameter d_{cross}, both the size d and the specific surface area S_{V_p} also uniquely characterize a fibre since

$$d_{\text{cross}} = \frac{4d}{S_{V_p} d - 2}. \tag{2}$$

Thus, we can, for example, express the volume V_{fibre} of a fibre as a function of size d and specific surface area S_{V_p} by

$$V_{\text{fibre}}(d, S_{V_p}) = \frac{\pi}{4} d_{\text{cross}}^2 d = \frac{4\pi d^3}{(S_{V_p} d - 2)^2}. \tag{3}$$